



OPEN ACCESS

EDITED BY

Noora Barzkar,
King Mongkut's University of Technology
North Bangkok, Thailand

REVIEWED BY

Lionel Ulmann,
Le Mans Université, France
Hongli Cui,
Shanxi Agricultural University, China

*CORRESPONDENCE

Shufang Yang
✉ shufang-yang@szu.edu.cn
Feng Chen
✉ sfchen@szu.edu.cn

RECEIVED 09 March 2023

ACCEPTED 17 May 2023

PUBLISHED 05 June 2023

CITATION

Lu X, Sun H, He Y, Yang S and Chen F
(2023) System metabolic tools reveal
fucoxanthin metabolism in *Nitzschia laevis*
for the improvement of fucoxanthin
productivity.
Front. Mar. Sci. 10:1182777.
doi: 10.3389/fmars.2023.1182777

COPYRIGHT

© 2023 Lu, Sun, He, Yang and Chen. This is
an open-access article distributed under the
terms of the [Creative Commons Attribution
License \(CC BY\)](https://creativecommons.org/licenses/by/4.0/). The use, distribution or
reproduction in other forums is permitted,
provided the original author(s) and the
copyright owner(s) are credited and that
the original publication in this journal is
cited, in accordance with accepted
academic practice. No use, distribution or
reproduction is permitted which does not
comply with these terms.

System metabolic tools reveal fucoxanthin metabolism in *Nitzschia laevis* for the improvement of fucoxanthin productivity

Xue Lu^{1,2,3}, Han Sun¹, Yongjin He⁴, Shufang Yang^{1*}
and Feng Chen^{1*}

¹Institute for Advanced Study, Shenzhen University, Shenzhen, China, ²Institute of New Materials and Advanced Manufacturing, Beijing Academy of Science and Technology, Beijing, China, ³Institute for Food and Bioresource Engineering, College of Engineering, Peking University, Beijing, China, ⁴College of Life Science, Fujian Normal University, Fuzhou, China

The production of fucoxanthin from microalgae is rapidly gaining popularity due to its exceptional productivity, lack of contamination, and straightforward extraction process. However, the optimal conditions for increasing biomass concentration and/or fucoxanthin content through the manipulation of light and carbon sources are context specific. This study explored fucoxanthin metabolism in *Nitzschia laevis* under heterotrophic and mixotrophic conditions using ¹³C tracer-based metabolic flux analysis, targeted metabolomics, and transcriptome analysis. Mixotrophic culture at 10 μmol m⁻² s⁻¹ improved fucoxanthin content by 27.54% but decreased biomass concentration by 15.65% compared to heterotrophic culture. At the molecular level, exposure to low light results in a reduction in carbon flux in the TCA cycle, leading to an increased flux toward carotenoid and fatty acid biosynthesis. The accumulation of high levels of citrate, isocitrate, and α-ketoglutaric acid is attributed to the reduced activity of the TCA cycle. Moreover, the metabolism of glyceraldehyde-3-phosphate and phosphoenolpyruvate was found to be more active under mixotrophic cultivation than heterotrophic ones, resulting in a substantial accumulation of fucoxanthin. The higher ATP and NADPH consumption provided sufficient energy for fucoxanthin and fatty acid biosynthesis. Furthermore, gene expression analysis revealed that low light upregulated the genes involved in fucoxanthin biosynthesis and promoted the violaxanthin cycle, especially after 12 h of cultivation. To improve fucoxanthin productivity, low light conditions were applied after a fed-batch culture, resulting in a 22.92% increase in fucoxanthin accumulation. The findings of this study offer valuable insights into the advantages of employing multi-stage cultivation techniques to improve microalgal production.

KEYWORDS

fucoxanthin, microalgae, carbon metabolism, low light intensity, fed-batch culture

1 Introduction

Fucoxanthin is mainly found in diatoms, which are distributed globally in the oceans and contribute ~20% of the global primary production (Sun et al., 2022). It is involved in the formation of the complex with chlorophyll a/c binding proteins (FCPs), which enhance the light-harvesting and photoprotective capabilities of diatoms. The FCPs attract significant attention in the field of biochemical characteristics due to their benefits for carbon fixation and global primary production. The crystal structure of FCPs has been studied to gain a deeper understanding of their functions (Wang et al., 2019). However, the metabolic pathway of fucoxanthin in diatoms remains unclear, despite its crucial role in FCPs. Recent studies revealed that fucoxanthin biosynthesis involves several steps, including isoprene biosynthesis, lycopene biosynthesis and cyclization, xanthophyll biosynthesis, and ultimately fucoxanthin biosynthesis (Mikami and Hosokawa, 2013; Li et al., 2022). The enzymes involved in the final step of biosynthesis are unclear, but the genomic analysis of *Phaeodactylum tricornutum* and *Thalassiosira pseudonana* suggests that violaxanthin and neoxanthin may serve as the final precursors for fucoxanthin biosynthesis (Sun et al., 2022).

Fucoxanthin is attracting increasing attention for its potential benefits in human health, such as preventive, protective, and therapeutic effects for a wide range of diseases (Zarekarizi et al., 2019). Microalgae are a viable source for fucoxanthin production due to their higher fucoxanthin productivity compared to macroalgae. This has led to a growing interest in the development of microalgae-based systems for the commercial production of fucoxanthin. The fucoxanthin content of *Isochrysis galbana* has been reported to be 1.2 to 15 times higher than that of macroalgae, and the content could reach 1.83% using a cheap and efficient extraction method (Kim et al., 2012). *P. tricornutum* is currently the best-studied marine diatom. It is notable for containing fucoxanthin as its primary carotenoid, which makes up approximately 1.57% of its total content. In a study by Wang et al. (2018), *P. tricornutum* and *Cylindrotheca fusiformis* were cultured for fucoxanthin production, and the yields obtained were 8.32 mg/L and 6.05 mg/L, respectively. Furthermore, it was found that *Cylindrotheca closterium* has the potential to accumulate fucoxanthin content up to 2.55% (Wang et al., 2018). *Nitzschia laevis* is a promising candidate for fucoxanthin production. Its maximum biomass for mixotrophic, heterotrophic, and photoautotrophic cultures was reported to be 2.27, 2.04, and 0.5 g/L, respectively (Wen and Chen, 2000). To improve fucoxanthin productivity, a fed-batch culture under heterotrophic mode was designed to greatly enhance *N. laevis* biomass to 17.25 g L⁻¹ (Lu et al., 2018). However, the mixotrophic culture of *N. laevis* resulted in significantly higher levels of fucoxanthin (60.12%) and eicosapentaenoic acid (EPA, C20:5) (50.67%) compared to the heterotrophic mode (Lu et al., 2019). Light has been shown to be beneficial for fucoxanthin accumulation in various species, including *P. tricornutum* and *I. zhangjiangensis* (Li et al., 2019; Yi et al., 2019). To improve productivity, it is important to understand the contribution of carbon sources and light to the fucoxanthin accumulation in *N. laevis*. However, the regulation of fucoxanthin biosynthesis under

mixotrophic conditions is complex and involves multiple metabolic pathways, including the Calvin–Benson–Bassham (CBB) cycle, the Embden–Meyerhof–Parnas (EMP) pathway, the pentose phosphate (PP) pathway, and the tricarboxylic acid (TCA) cycle (Sun et al., 2022).

Nowadays, systemic metabolic tools have been developed to investigate the dynamic metabolism of target products (Sun et al., 2021). In the process of fucoxanthin biosynthesis, various factors such as the metabolic flux of central carbon metabolism, gene expression of the synthetic pathway, and intermediate metabolites play a crucial role in the fucoxanthin accumulation in *N. laevis*. However, it is still unclear whether metabolic flux or metabolite content is the primary limiting factor for fucoxanthin production. Identifying the limiting factor may help develop targeted cultivation strategies to improve fucoxanthin yield. A previous study suggested that elevated carbon availability was favorable for astaxanthin biosynthesis under stress conditions; then, fed-batch culture without a nitrogen source was applied to improve astaxanthin productivity to 2.0 mg L⁻¹ d⁻¹ (Sun et al., 2020b). Similarly, the key factors for fucoxanthin biosynthesis in mixotrophic mode are heuristics for fucoxanthin production by different strategies, including fed-batch culture and multistage culture. As an efficient tool, metabolic flux analysis calculates the cell metabolic network and identifies the potential products of metabolic engineering. Transcriptomics analyzes cell metabolism at the level of gene expression patterns and identifies transcriptional regulators of targeted products. Targeted metabolomics is the detection and analysis of specific groups of metabolites to identify the key metabolite (Sun et al., 2021). The combination and optimization of multiple metabolic tools can quantitatively and dynamically describe fucoxanthin biosynthesis in different modes.

This study was designed to investigate the metabolism of *N. laevis* growth and fucoxanthin biosynthesis in heterotrophic and mixotrophic modes. First, low light at 10 μmol m⁻² s⁻¹ was used to induce fucoxanthin accumulation by influencing cell growth and carotenoid and fatty acid profiles. Then, ¹³C tracer-based metabolic flux analysis (¹³C-MFA) was designed to map the carbon flux of *N. laevis* in different modes. Targeted metabolomics was applied to focus on the metabolite changes in central carbon metabolism. Third, the genes involved in fucoxanthin biosynthesis were also annotated and analyzed by transcriptomics. Finally, low light was applied to induce fucoxanthin accumulation for 12 h or 24 h after fed-batch culture, depending on the molecular level. This study is instructive and valuable for exploring fucoxanthin metabolism and can provide various strategies for fucoxanthin production.

2 Materials and methods

2.1 Batch culture of *Nitzschia laevis*

The *Nitzschia laevis* UTEX 2047 was purchased from the Culture Collection of Algae at the University of Texas – Austin, USA. *N. laevis* was cultured in the modified LDM medium (per L) consisting of salt 20 g, glucose 5 g, NaNO₃ 0.68 g, Na₂SiO₃·9H₂O 120 mg, K₂HPO₄ 7.5 mg, KH₂PO₄ 17.5 mg, MgSO₄·7H₂O 7.5 mg,

Na₂EDTA 4.5 mg, CaCl₂·2H₂O 2.5 mg, FeCl₃·6H₂O 0.582 mg, ZnCl₂ 0.03 mg, CoCl₂·6H₂O 0.012 mg, Na₂MoO₄·2H₂O 0.024 mg, MnCl₂·4H₂O 0.246 mg, biotin 0.025 mg, VB₁₂ 0.015 mg. The medium was adjusted to pH 8.5 and then autoclaved at 121°C for 20 min.

Before inoculation, the microalgal seeds were observed under a microscope to check for bacterial contamination. If there was no contamination, the 10 mL cell suspension was centrifuged in a 50 mL sterile centrifuge tube (430829, Corning) at 3,000 g for 5 min and the cells were collected in a clean bench. Then the cell pellet was resuspended twice in fresh medium and transferred to 250 mL Erlenmeyer flasks containing 100 mL of fresh medium in the clean bench. A total of 1 mL of microalgae solution was taken, and cells were observed under a microscope to ensure that there was no bacterial contamination before proceeding with subsequent experiments. The light intensity was set to 0, 10, and 60 μmol m⁻² s⁻¹ to explore its effect on cell growth and fucoxanthin accumulation, with the light cycle set to 24: 0. Cells were cultured at 23°C with orbital shaking at 150 rpm.

2.2 Heterotrophic fed-batch culture of *Nitzschia laevis*

In the exponential growth phase of *N. laevis*, the general assumption was that substance and energy consumption for cell maintenance were low and that extracellular products were rarely produced. The model was established based on a previous study in 250-mL Erlenmeyer flasks (Sun et al., 2020b). The fed-batch medium (per L) consisted of glucose 500.0 g, NaNO₃ 113.4 g, and KH₂PO₄ 16.6 g, according to our previous study (Lu et al., 2018). The *N. laevis* was cultured in heterotrophic fed-batch mode for 7 days. Other conditions were the same as in the batch culture. Finally, after 7 days of fed-batch culture, light at 10 μmol m⁻² s⁻¹ was applied to induce fucoxanthin accumulation for 12 h or 24 h. The total cultivation period was 7.5 or 8 days.

2.3 ¹³C tracer-based metabolic flux analysis

¹³C-MFA was calculated based on the biomass components by establishing the biomass reaction. Samples were dissolved in tetrahydrofuran and derivatized at 85°C with *N*-tert-butyltrimethylsilyl-*N*-methyltrifluoroacetamide. The derivatives were analyzed by GC-MS (7890B-5977B, Agilent). The abundance of labeled amino acids was modified by removing the statistical weight of CO₂, which was analyzed by 100% U-¹³C glucose. The metabolic network reaction in the Metran software was set according to a previous study (Sun et al., 2020a). Samples of amino acids with varying abundances were processed using the Metran software for metabolic flux analysis. The software analyzed the ¹³C labeling abundance of the amino acids, which was then used to calculate the designated metabolic network flux (Yoo et al., 2008; Zhao et al., 2015).

In the ¹³C-MFA, it was necessary to establish a formula for the composition of cell biomass under different culture conditions. The main components of biomass include amino acids, polysaccharides,

fatty acids, pigments, nucleic acids, and other ash contents. The measurement methods can be found in Section 2.8. Therefore, the composition of heterotrophic and mixotrophic *N. laevis* cells was determined and converted to 1 mol C per chemical formula (Yoo et al., 2008; Sun et al., 2021). In addition, *N. laevis* contained various polyunsaturated fatty acids (PUFAs), which were set in the network reaction (Wen and Chen, 2000). Therefore, the *N. laevis* biomass in heterotrophic mode was calculated as follows: Biomass+9.583197 ADP = 0.056402 rCTP+0.056402 rGTP+0.053848 rATP+0.053848 rUTP+9.583197 ATP+0.035019 dGTP+0.035019 dCTP+0.033434 dATP+0.033434 dTTP+0.033216 C16:0 + 0.052794 C16:1 + 0.007746 C16:2 + 0.006107 C18:0 + 0.002692 C18:1 + 0.003656 C18:2 + 0.007304 C18:3 + 0.002764 C18:4 + 0.006056 C20:4 + 0.046881 C20:5 + 0.003226 C22:6 + 2.071138 ADPG+0.314001 Asp +0.167500 Thr+0.184735 Ser+0.347416 Glu+0.209890 Gly +0.271960 Ala+0.083180 Cys+0.188983 Val+0.007741 Met +0.114992 Ile+0.067402 Tyr+0.203198 Leu+0.105983 Phe +0.185072 Lys+0.044370 His+0.305733 Arg+0.100380 Pro +0.198718 Glyc3P+0.021261 DOXP. If the biomass component under mixotrophic mode differed from that under heterotrophic mode, then the biomass in mixotrophic mode was as follows: Biomass+6.983670 ADP = 0.065550 rCTP+0.065550 rGTP +0.062582 rATP+0.062582 rUTP+6.983670 ATP+0.036841 dGTP +0.036841 dCTP+0.035173 dATP+0.035173 dTTP+0.034440 C16:0 + 0.067289 C16:1 + 0.013147 C16:2 + 0.007592 C18:0 + 0.002491 C18:1 + 0.003742 C18:2 + 0.003637 C18:3 + 0.003218 C18:4 + 0.005899 C20:4 + 0.061147 C20:5 + 0.005016 C22:6 + 1.442191 ADPG+0.544806 Asp+0.267555 Thr+0.286010 Ser+0.007295 Gln +0.616866 Glu+0.321639 Gly+0.419399 Ala+0.132279 Cys +0.288999 Val+0.030911 Met+0.174103 Ile+0.096793 Tyr +0.305978 Leu+0.145326 Phe+0.355389 Lys+0.067688 His +0.568539 Arg+0.161666 Pro+0.239052 Glyc3P+0.027708 DOXP.

2.4 Metabolite extraction and analysis

Fresh microalgae were centrifuged at 5,000 g for 5 min at 4°C, and the supernatant was discarded. The cells were resuspended in 80% (v/v, methanol/water) pre-cooled methanol, immediately frozen in liquid nitrogen, and then incubated at -20 °C for 30 min, which could inhibit the activation of lipase. Then the samples were centrifuged at 4 °C for 15 min at 15,000 g to save the supernatant. The extraction process was performed three times to collect the supernatants before detection by UPLC-MS/MS (Waters, Milford, MA, USA). The HPLC analysis was performed on an HSS T3 column (C18, 2.1 mm × 100 mm, 1.8 μm, Waters), mobile phase A: methanol: isopropanol (68:32, v/v, 0.1% formic acid), mobile phase B: acetonitrile: methanol: water (84:2:14, v/v/v, 0.1% formic acid). The flow rate was set at 0.4 mL/min, the column temperature was set at 40°C, the sample chamber was set at 4°C, and the injection volume was 1 μL. Mass spectrometry analysis was performed using SYNAPT G2-Si (Waters), the ion source temperature was 100 °C, the capillary voltage was 1.5 kV, the cone-hole voltage was 30 V, the desolvation gas was 800 L/h, the desolvation temperature was 500 °C, the mass scanning range was m/z 100-1200, and the collection speed was 1.5 scan/s.

2.5 RNA extraction and RNA-seq analysis

Cells at 6 h, 12 h, 24 h, and 48 h in the dark and low light were collected and immediately stored in liquid nitrogen for RNA extraction. The mortar was pre-cooled, and the algae cells were then ground to a powder using liquid nitrogen. RNA extraction was performed according to the instructions of the plant RNA extraction kit. Finally, the RNA concentration was determined using a UV spectrophotometer. The RIN value, 28S/18S, and concentration were detected by the Agilent bioanalyzer. The values of OD260/OD280 and OD260/OD230 were determined to evaluate the purity of the samples.

2.6 Differential gene expression analysis

The filtered reads were aligned to the reference gene sequence obtained by third-generation sequencing using Bowtie2, and then RSEM software was used to calculate gene expression levels from the RNA-seq data. The PCA was performed using princomp. Finally, the identified DEGs (differentially expressed genes) between samples were clustered using Deseq2 software, with a fold change ≥ 2.00 , and an adjusted p -value (P_{adj}) ≤ 0.001 . Mfuzz was used for time-series analysis based on the relaxed clustering algorithm.

2.7 Expression levels of mRNA

Total RNA was extracted using RNA Plant Plus Reagent (Tiangen, Beijing, China). Then, 1 μg of extracted RNA was used for reverse transcription to cDNA using the QuantScript RT Kit reagent. Real-time PCR was performed using SYBR premix Ex Taq. The relative expression of Ct values in each reaction was calculated, and the actin gene was used as an internal reference for normalization.

2.8 Experimental methods

2.8.1 Determination of biomass

The biomass concentration was monitored by gravimetry as the dry cell weight. The culture medium (1 mL) was centrifuged at 5,000 g for 5 min. Sediment pellets were washed and filtered with dry, pre-weighed filter paper, then dried at 60°C in a vacuum oven to a constant weight. Thereafter, the samples were cooled and weighed. Biomass was expressed as the ratio of the dry weight of cells to the volume of the medium (g L^{-1}).

2.8.2 Determination of fucoxanthin content

Microalgal cells were centrifuged for harvesting and freeze-dried in a vacuum freeze dryer. The 10 mg lyophilized algae powder was extracted with ethanol until the cells were colorless. Then the supernatant was collected at 5000 g for 5 min and dried by a stream of nitrogen gas. The dried extract was re-dissolved in 1 mL of ethanol and filtered through a 0.22- μm Millipore membrane. All operations were conducted under conditions of light avoidance. The

fucoxanthin content was analyzed by high-performance liquid chromatography (HPLC).

2.8.3 Determination of pigment composition

Cell pellets were dissolved in 99.9% methanol and incubated at 45°C in the dark for 24 h. The mixture was centrifuged, and the absorbance of the supernatant was measured separately at 470, 652.4, and 665.2 nm. Pigment concentrations were calculated according to the previous study (Chokshi et al., 2017).

2.8.4 Determination of fatty acid composition

The biomass was extracted using chloroform and methyl alcohol. The chloroform layer was esterified to fatty acid methyl esters (FAMES) by incubation with 1% sulfuric acid in methanol. FAMES were analyzed using a GC-MS (Shimadzu, Kyoto, Japan) equipped with an Rtx-2330 capillary column (30 m \times 0.25 mm \times 0.25 μm) (Restek, Guangzhou, China). The operating parameters were set according to a previous study (Liu et al., 2016).

2.8.5 Determination of ROS levels

The levels of intracellular ROS were determined by measuring the oxidative conversion of 2', 7'-dichlorodihydrofluorescein diacetate (DCFH-DA) to the strong fluorescent product 2', 7'-dichlorofluorescein (DCF) using the ROS kit (Beyotime Institute of Biotechnology, China) (Wang et al., 2023). The 1 mL of cell solution was centrifuged at 13000 g for 3 min, and the supernatant was discarded. Then, the 500 μL of 10 μM DCFH-DA was added to the cell pellet. After 20 min of incubation, the cells were washed twice with deionized water, then 1 mL of deionized water was added and mixed thoroughly. The absorbance value of the cells at 525 nm was measured with a microplate reader under excitation light at 488 nm to calculate ROS levels.

2.8.6 Measurement of F_v/F_m

The 3 mL of cell solution was collected in the dark for 20 min to adapt to the dark environment. The primary light energy conversion efficiency of PS II (F_v/F_m) was determined by pulse-amplitude-modulated (PAM) fluorometry (Walz, Effeltrich, Germany).

2.9 Statistical analysis

All experiments were conducted in at least three replicates to ensure reproducibility. Data were statistically analyzed using SPSS software and one-way analysis of variance (ANOVA) with *post hoc* multiple-comparison least significant difference (LSD) tests to detect significant differences.

3 Results and discussion

3.1 Light improves fucoxanthin content

As shown in Figure 1, cell growth and fucoxanthin accumulation were investigated in different modes. The biomass concentration

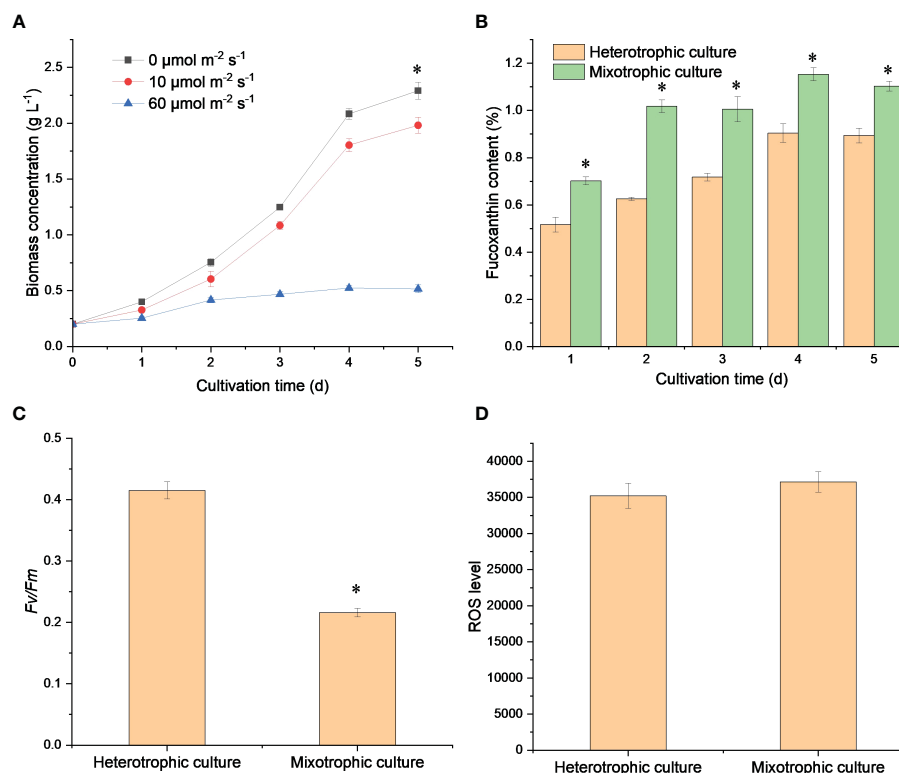


FIGURE 1

Growth profiles (A), fucoxanthin content (B), F_v/F_m (C), and ROS levels (D) of *N. laevis* under heterotrophic and mixotrophic modes. Asterisks indicate a significant difference between the two culture modes ($p < 0.05$), $N = 3$.

under heterotrophic mode was significantly higher than that at 10 $\mu\text{mol m}^{-2} \text{s}^{-1}$ ($p = 0.00096$) and 60 $\mu\text{mol m}^{-2} \text{s}^{-1}$ ($p = 0.00000040$), which is promising to realize the high-cell density of *N. laevis* by overcoming the lack of available photons in each cell (Perez-Garcia et al., 2011). A previous study also indicated that the specific growth rate of *N. laevis* under heterotrophic mode (0.684 ± 0.030) was higher than that under mixotrophic mode (0.584 ± 0.018) (Lu et al., 2019), which was mainly attributed to the potential conflicts between photosynthetic carbon fixation and glucose metabolism (Zhang et al., 2021). When the light intensity was increased to 60 $\mu\text{mol m}^{-2} \text{s}^{-1}$, the biomass concentration decreased to 0.52 g L^{-1} . However, the light intensity of 10 $\mu\text{mol m}^{-2} \text{s}^{-1}$ improved the fucoxanthin accumulation significantly ($p = 0.00053$) higher than that under heterotrophic mode after 5 days of cultivation. The highest fucoxanthin content of 1.15% was obtained under 10 $\mu\text{mol m}^{-2} \text{s}^{-1}$ after 4 days of cultivation, which was 1.28-fold of that under dark conditions. Although the heterotrophic mode could improve the biomass of *N. laevis* by overcoming the light limitation, the low fucoxanthin content was the limiting factor for fucoxanthin production. In addition, low light reduced the F_v/F_m value to 0.216, which was 92.1% lower ($p = 0.00002$) than that in the dark condition. Since F_v/F_m is an indicator of the maximum photochemical efficiency of PS II, its decrease indicated that light limited the photosynthetic efficiency of *N. laevis* (Zhang et al., 2017). The potential conflict between light and glucose in *N. laevis* growth is an interesting phenomenon that is instructive in achieving the transition between different growth modes (Zhang et al., 2021). At the molecular level,

tackling the challenge of light-induced cell growth inhibition while promoting fucoxanthin accumulation is essential for achieving scalable production of fucoxanthin. The ROS levels of *N. laevis* under the two modes had no significant differences ($p = 0.20$), which was mainly attributed to the different contributions of respiration and photosynthesis.

3.2 Light influences carotenoid and fatty acid metabolism

Fucoxanthin is usually the largest proportion of carotenoids in diatom cells (Peng et al., 2011). As seen in Figure 2A, fucoxanthin accounted for about 80% of the total carotenoid and exhibited a fine linear relationship with carotenoids, which suggested that the improved carotenoid content was mainly due to massive fucoxanthin accumulation (Figure 2B). Fucoxanthin, chlorophyll a, and chlorophyll c can trap photoelectrons for efficient energy transfer and dissipation (Wang et al., 2020). Therefore, light could promote sufficient carbon molecules for fucoxanthin biosynthesis through the CBB cycle, which in turn improved the photosynthetic efficiency for cell growth. However, *N. laevis* cells grew rapidly under dark conditions, which suggested the presence of potential carbon metabolism conflicts between the EMP pathway and CBB cycle, which limited *N. laevis* growth under mixotrophic mode.

In addition, the mixotrophic mode increased the lipid and EPA content (Lu et al., 2019). As shown in Table 1, the C16:0, C16:1,

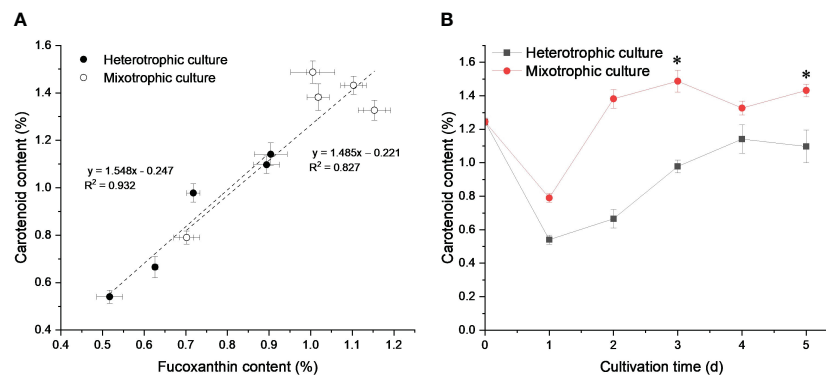


FIGURE 2

Linear relationship between carotenoid and fucoxanthin content (A), and carotenoid profiles (B) under heterotrophic and mixotrophic modes. Asterisks indicate a significant difference between the two culture modes ($p < 0.05$), $N = 3$.

and EPA content contained large portions of the fatty acid composition. Under heterotrophic culture, the fatty acid content, except for C16:0 and C18:4, increased with time. The content of C16:1 and EPA could reach 2.97% and 2.28%, respectively. The total fatty acid content also showed an upward trend, which greatly

increased after 3 days of cultivation and finally reached 9.99%. Under mixotrophic culture, the fatty acids increased during the first 2 days of cultivation and slightly decreased in the late logarithmic phase. The highest content of 13.83% was obtained after 5 days of cultivation. Therefore, low light was beneficial for fatty acid

TABLE 1 The fatty acid profiles of *N. laevis* under heterotrophic and mixotrophic culture ^a.

Fatty acids (g per 100 g of biomass)	Heterotrophic culture					Mixotrophic culture				
	1d	2d	3d	4d	5d	1d	2d	3d	4d	5d
C14:0	0.75 ± 0.05	0.75 ± 0.04	0.94 ± 0.11	0.90 ± 0.06	0.76 ± 0.02	0.65 ± 0.01	1.00 ± 0.09	0.84 ± 0.06	0.90 ± 0.05	1.26 ± 0.14
C16:0	1.93 ± 0.13	1.77 ± 0.04	1.63 ± 0.28	1.45 ± 0.09	1.28 ± 0.06	1.55 ± 0.02	2.39 ± 0.20	1.89 ± 0.09	1.65 ± 0.09	2.13 ± 0.21
C16:1	1.89 ± 0.14	2.10 ± 0.05	2.85 ± 0.32	2.97 ± 0.17	2.80 ± 0.14	1.78 ± 0.02	2.53 ± 0.05	2.71 ± 0.25	3.22 ± 0.18	3.70 ± 0.43
C16:2*	0.22 ± 0.01	0.25 ± 0.03	0.38 ± 0.01	0.45 ± 0.03	0.45 ± 0.03	0.32 ± 0.01	0.82 ± 0.06	0.67 ± 0.01	0.63 ± 0.04	0.75 ± 0.06
C18:0	0.15 ± 0.05	0.18 ± 0.03	0.25 ± 0.02	0.27 ± 0.03	0.30 ± 0.01	0.16 ± 0.01	0.31 ± 0.05	0.35 ± 0.03	0.36 ± 0.02	0.43 ± 0.03
C18:1	0.16 ± 0.01	0.13 ± 0.01	0.13 ± 0.01	0.19 ± 0.01	0.19 ± 0.02	0.13 ± 0.01	0.19 ± 0.01	0.12 ± 0.02	0.12 ± 0.00	0.21 ± 0.02
C18:2	0.15 ± 0.01	0.14 ± 0.00	0.18 ± 0.02	0.19 ± 0.00	0.19 ± 0.01	0.14 ± 0.01	0.23 ± 0.01	0.19 ± 0.01	0.18 ± 0.01	0.22 ± 0.02
C18:3	0.17 ± 0.01	0.22 ± 0.01	0.30 ± 0.00	0.32 ± 0.02	0.35 ± 0.02	0.08 ± 0.01	0.15 ± 0.01	0.17 ± 0.00	0.17 ± 0.02	0.20 ± 0.01
C18:4	0.19 ± 0.00	0.15 ± 0.01	0.14 ± 0.01	0.12 ± 0.01	0.10 ± 0.01	0.14 ± 0.01	0.26 ± 0.02	0.23 ± 0.00	0.15 ± 0.01	0.15 ± 0.01
C20:4	0.11 ± 0.01	0.18 ± 0.01	0.30 ± 0.05	0.34 ± 0.03	0.32 ± 0.01	0.16 ± 0.00	0.51 ± 0.04	0.35 ± 0.03	0.28 ± 0.00	0.31 ± 0.03
C20:5 (EPA)*	1.11 ± 0.09	1.40 ± 0.10	1.90 ± 0.33	2.07 ± 0.11	2.28 ± 0.10	1.32 ± 0.06	2.52 ± 0.04	2.83 ± 0.03	2.93 ± 0.13	3.43 ± 0.24
Other fatty acids	0.59 ± 0.04	0.60 ± 0.04	0.68 ± 0.04	0.72 ± 0.08	0.72 ± 0.08	0.56 ± 0.04	1.02 ± 0.06	0.88 ± 0.06	0.84 ± 0.08	1.06 ± 0.07
Total fatty acids*	7.42 ± 0.35	7.87 ± 0.18	9.68 ± 0.66	9.99 ± 0.23	9.73 ± 0.35	6.99 ± 0.15	11.92 ± 0.38	11.24 ± 0.36	11.46 ± 0.41	13.83 ± 0.56

^aAsterisks indicate a significant difference between two culture modes ($p < 0.05$), $N = 3$.

biosynthesis in *N. laevis*, especially the EPA. Low light was reported to increase EPA content in *N. laevis* by 50.4% compared to heterotrophic cultivation (Lu et al., 2019), which was a promising strategy for EPA production. The PUFAs, including EPA, play a crucial role in the formation of cell membrane structure. These fatty acids are also closely linked to photon absorption and are believed to have an impact on the process of photosynthesis (Lu et al., 2019). Therefore, EPA biosynthesis in *N. laevis* had a good response to low light.

3.3 Light elevates metabolic flux in carotenoid and fatty acid metabolism

Light influenced the metabolic flux of the central carbon metabolism of *N. laevis* (Figure 3). Under mixotrophic culture, the flux to the PP pathway was improved to provide sufficient NADPH for lipid biosynthesis (Xue et al., 2017). The flux to carbohydrates was limited, but more flux was directed to the EMP pathway, TCA cycle, carotenoid metabolism, and fatty acid metabolism than in heterotrophic cultures. The G3P and its subsequent product PYR can react to produce DOXP, which is the first and most important step in the MEP pathway to produce a terpenoid skeleton (Gong and Bassi, 2016). The mixotrophic culture increased the flux to the MEP pathway by nearly 10%, thus providing more precursors for carotenoid biosynthesis. For lipid biosynthesis, the acetyl-CoA can generate the C16:0 and C18:0 through the condensation reaction. The carbon flux from acetyl-CoA to C16:0 and C18:0 was close under two culture modes, which indicated that light enhancement of fatty acid biosynthesis was mainly to promote acetyl-CoA production rather than the extension reaction of the fatty acid carbon chain. In addition, light limited the flux of the TCA cycle, but improved the anaplerotic reaction. As a consequence, the reduced source of ATP may have led to lower biomass concentrations compared to those observed in heterotrophic cultures. However, the flux distribution between PEP and OAA was improved to provide the precursors for carotenoid and fatty acid biosynthesis.

Since ^{13}C -MFA revealed the carbon flux during the exponential growth phase, the metabolite changes on days 2 and 4 were evaluated. As shown in Table 2, the G6P and F6P content had no significant difference between the two modes. The G3P and PEP metabolism under the mixotrophic mode was higher than that under the heterotrophic mode, which contributed to the massive accumulation of fucoxanthin. The higher PYR on day 4 was mainly attributed to the improved flux from OAA to PEP. These results suggested that low light tended to induce available carbon into carotenoid biosynthesis. During the TCA cycle, CIT ($p = 0.017$), ICT ($p = 0.0024$), and AKG ($p = 0.000010$) were higher on day 4 under the mixotrophic mode, which was consistent with ^{13}C -MFA. The limited flux of the TCA cycle blocked their reactions. In addition, NADPH and ATP metabolism were higher in the mixotrophic mode than in the heterotrophic mode, resulting in high fucoxanthin and fatty acid contents.

3.4 Light up-regulates genes involved in fucoxanthin and fatty acid biosynthesis

As shown in Figure 4A, most of the genes involved in the MEP pathway and the carotenoid biosynthetic pathway were up-regulated, especially at 12 h. The precursors of carotenoids in microalgae mainly come from the MEP pathway (Gong and Bassi, 2016), so the expression of the key genes in the MEP pathway determines the synthetic efficiency. The *DXR*, *CMS*, *CMK*, *HDS*, and *HDR* in the MEP pathway were up-regulated at 12 h, but the *CMK* and *HDS* were down-regulated after 12 h, indicating that low light began to regulate carotenoid metabolism within 12 h. At 48 h, the *GPPS* and *GGPPS*, which were involved in phytoene production from DMAPP, were down-regulated. After 24 h, low-light treatment no longer exhibited any significant effects on carotenoid biosynthesis at the genetic level. The up-regulated genes at 12 h encouraged more PYR to produce DMAPP for carotenoid biosynthesis. The GGPP produces phytoene through *PSY* and lycopene through *PDS*, *Z-ISO*, *ZDS*, and *CRTISO*, which were up-regulated at low light. Antheraxanthin, violaxanthin, and zeaxanthin were interconverted by *ZEP* and *VDE* to form the violaxanthin cycle. Both *ZEP* and *VDE* were up-regulated under low light, indicating that low light promotes the violaxanthin cycle.

As shown in Figure 4B, the expression level of the *ACC*ase gene was up-regulated under mixotrophic culture at 12 h. Malonyl-CoA was converted to malonyl-ACP by the action of *MCT*. Under the catalytic action of *KAS*, *KAR*, *HAD*, and *ENR*, malonyl-ACP went through cycles of condensation, reduction, dehydration, and reduction to produce C16:0-ACP or C18:0-ACP. The up-regulation of *KAS*, *KAR*, and *ENR* revealed that low light promoted fatty acid biosynthesis after 12 h of cultivation. The C16:0-ACP was able to form C18:0 under the action of *ELO* and *HACD* and then formed C18:1 under the action of Δ^9 desaturase. The C18:0 was also able to produce the C18:2 by *SAD* and $\Delta^{12}\text{FAD}$. Their up-regulation suggests that low light promotes C18:1 and C18:2 biosynthesis.

3.5 Light induces fucoxanthin accumulation after high cell density

Low light improved fucoxanthin biosynthesis but limited the carbon flux of the TCA cycle, inhibiting *N. laevis* growth. As shown in Figure 5A, the heterotrophic fed-batch culture was designed to increase the biomass concentration to 6.07 g L^{-1} for 7 days, which is 3.0-fold of the batch culture. Adequate nutrient availability facilitated rapid cell growth. Under dark conditions, carbon flux tended to participate in the TCA cycle to produce amounts of ATP for cell growth, but the flux to fatty acid and carotenoid metabolism was limited. Since the genes involved in fucoxanthin biosynthesis were mostly up-regulated at 12 h, the light was then applied to induce fucoxanthin accumulation for 12 h and 24 h. As shown in Figure 5B, the fucoxanthin content under 12 h ($p = 0.000012$), 24 h ($p = 0.000073$), and 48 h ($p = 0.000034$) light treatment was 1.08%, 1.03%, and 1.05%, respectively, which was significantly ($p < 0.05$)

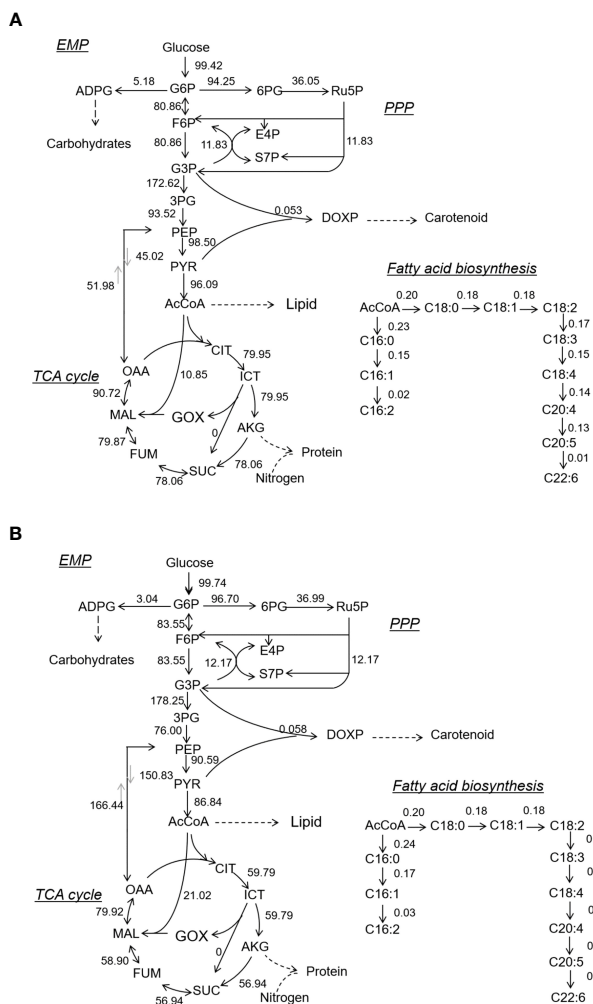


FIGURE 3 Metabolic flux of central carbon metabolism and fatty acid biosynthesis in *N. laevis* under heterotrophic (A) and mixotrophic (B) modes. The carbon metabolites: G6P, glucose-6-phosphate; F6P, fructose-6-phosphate; GAP, glyceraldehyde-3-phosphate; 3PG, 3-phospho-D-glycerate; PEP, phosphoenolpyruvate; PYR, pyruvate; AcCoA, acetyl-coenzyme A; 6PG, 6-phospho-D-gluconate; Ru5P, ribulose-5-phosphate; E4P, erythrose-4-phosphate; S7P, sedoheptulose-7-phosphate; CIT, citrate; ICIT, isocitrate; AKG, α -ketoglutarate; SUC, succinate; FUM, fumarate; MAL, malate; and OAA, oxaloacetate.

TABLE 2 LC-MS results for various metabolites of *N. laevis* in heterotrophic and mixotrophic modes.

Metabolite (ug/g)	Heterotrophic mode			Mixotrophic mode	
	d0	d2	d4	d2	d4
EMP and PP pathways					
G6P	94.9 ± 7.5	134.4 ± 12.2	54.9 ± 5.0	156.4 ± 10.7	56.7 ± 7.4
F6P	98.9 ± 10.6	122.5 ± 14.1	62.7 ± 8.7	116.2 ± 12.2	67.1 ± 17.0
G3P	114.5 ± 157	2593 ± 122	2119 ± 204	5385 ± 239	1460 ± 67.2
3PGA	88.2 ± 14.6	106.5 ± 8.9	714.6 ± 63.4	145.2 ± 15.0	516.0 ± 44.3
6PG	19.9 ± 0.8	6.1 ± 0.4	2.1 ± 0.1	4.3 ± 0.1	11.1 ± 13.0
PEP	12.5 ± 1.5	6.0 ± 2.8	6.7 ± 1.2	15.5 ± 0.9	4.9 ± 0.9
PYR	71.3 ± 4.1	56.9 ± 4.8	23.7 ± 4.9	68.9 ± 9.5	74.2 ± 4.2
TCA cycle					
Acce-CoA	126.0 ± 3.1	122.9 ± 7.7	20.7 ± 5.1	183.9 ± 15.2	10.2 ± 0.7

(Continued)

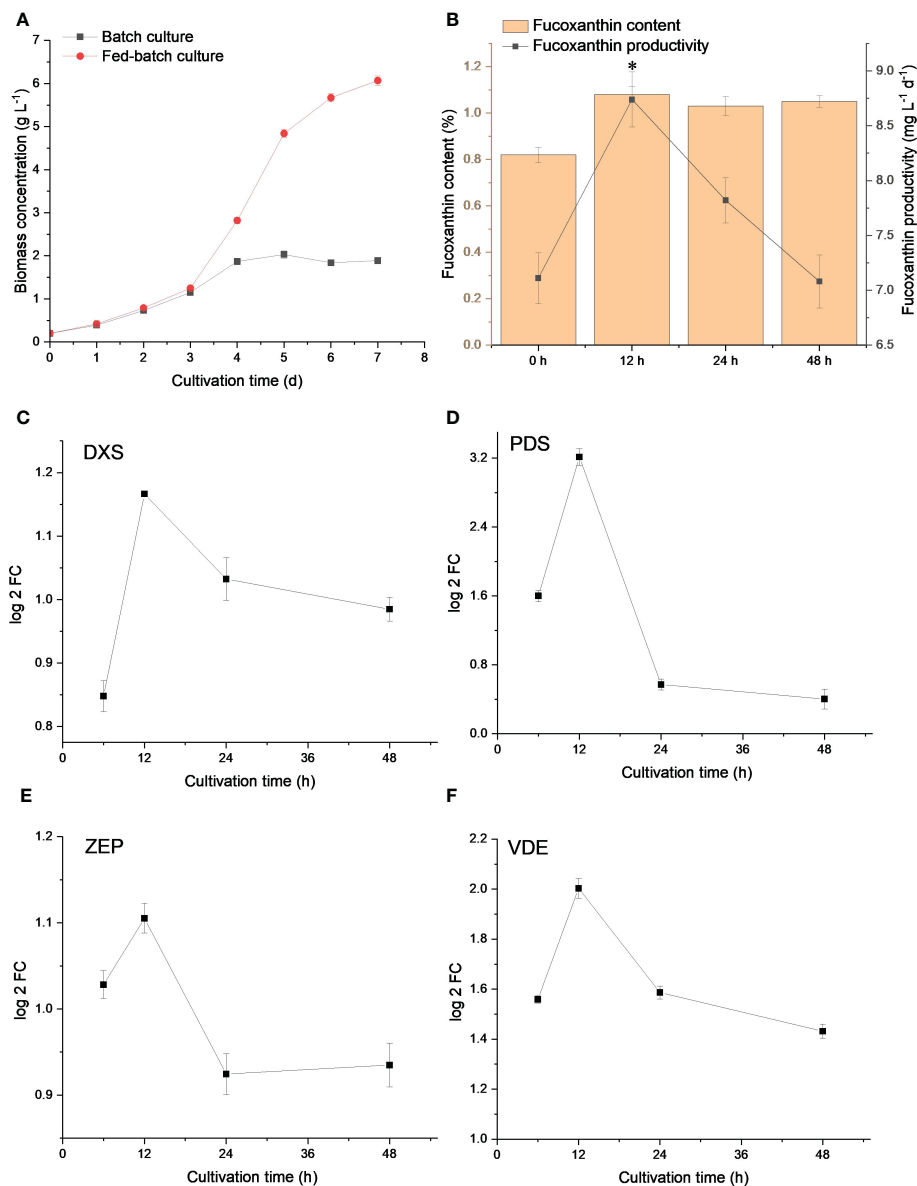


FIGURE 5

Biomass concentration of *N. laevis* under batch and fed-batch culture (A), and fucoxanthin content and productivity (B) under different light treatments. Expression levels of *DXS* (C), *PDS* (D), *ZEP* (E), and *VDE* (F) under different light treatments. The asterisks indicate a significant difference between 0 and 12 h ($p < 0.05$), $N = 3$.

higher than that in the dark condition. Although the light treatment prolonged the cultivation time for 12 h ($p = 0.000029$) and 24 h ($p = 0.006513$), the fucoxanthin productivity was significantly improved and reached the highest value of $8.74 \text{ mg L}^{-1} \text{ d}^{-1}$ at 12 h.

The expression levels of related genes revealed that *DXS*, *PDS*, *ZEP*, and *VDE* were up-regulated at 12 h (Figures 5C–F), but *PDS* and *ZEP* were down-regulated at 24 h. The expression level of these genes was further decreased at 48 h. The prolonged light induction was not efficient for fucoxanthin biosynthesis. Light treatment for 12 h was conducive to improving fucoxanthin productivity at the gene level. Taken together, the system metabolic tools revealed the fucoxanthin metabolism at the molecular level and could provide various strategies for fucoxanthin production.

4 Conclusions

The mixotrophic mode limited *N. laevis* growth but improved fucoxanthin accumulation as compared to the heterotrophic mode. Low light was disadvantageous for glucose metabolism as it suppressed the carbon flux of the TCA cycle, which was the main reason for the low biomass concentration. Low light tended to increase carbon flux toward fucoxanthin and fatty acid biosynthesis by improving the carbon flux and up-regulating related genes, especially at 12 h. The improved ATP and NADPH in the mixotrophic mode provide sufficient energy for fucoxanthin biosynthesis. Finally, low light was applied to improve fucoxanthin productivity by 22.92% after a fed-batch culture.

Data availability statement

The data presented in the study are deposited in the NCBI repository, accession number PRJNA975947.

Author contributions

XL: conceptualization, methodology, data curation. HS: conceptualization, methodology, software. YH: data curation, investigation. SY: data curation, writing - original draft preparation, funding, writing- reviewing and editing. FC: conceptualization, writing - reviewing and editing. All authors contributed to the article and approved the submitted version.

Funding

This research was financially supported by the Guangdong Province Zhujiang Talent Program (2019ZT08H476), the Science

References

- Chokshi, K., Pancha, I., Ghosh, A., and Mishra, S. (2017). Nitrogen starvation-induced cellular crosstalk of ROS-scavenging antioxidants and phytohormone enhanced the biofuel potential of green microalga *acutodesmus dimorphus*. *Biotechnol. Biofuels* 10, 60. doi: 10.1186/s13068-017-0747-7
- Gong, M., and Bassi, A. (2016). Carotenoids from microalgae: a review of recent developments. *Biotechnol. Adv.* 34 (8), 1396–1412. doi: 10.1016/j.biotechadv.2016.10.005
- Kim, S. M., Kang, S.-W., Kwon, O. N., Chung, D., and Pan, C.-H. (2012). Fucoxanthin as a major carotenoid in *isochrysis aff. galbana*: characterization of extraction for commercial application. *J. Korean Soc. Appl. Biol. Chem.* 55 (4), 477–483. doi: 10.1007/s13765-012-2108-3
- Li, Y., Sun, H., Wang, Y., Yang, S., Wang, J., Wu, T., et al. (2022). Integrated metabolic tools reveal carbon alternative in *isochrysis zhangjiangensis* for fucoxanthin improvement. *Bioresource Technol.* 347, 126401. doi: 10.1016/j.biortech.2021.126401
- Li, Y., Sun, H., Wu, T., Fu, Y., He, Y., Mao, X., et al. (2019). Storage carbon metabolism of *isochrysis zhangjiangensis* under different light intensities and its application for co-production of fucoxanthin and stearidonic acid. *Bioresource Technol.* 282, 94–102. doi: 10.1016/j.biortech.2019.02.127
- Liu, J., Han, D., Yoon, K., Hu, Q., and Li, Y. (2016). Characterization of type 2 diacylglycerol acyltransferases in *chlamydomonas reinhardtii* reveals their distinct substrate specificities and functions in triacylglycerol biosynthesis. *Plant J.* 86 (1), 3–19. doi: 10.1111/tpj.13143
- Lu, X., Liu, B., He, Y., Guo, B., Sun, H., and Chen, F. (2019). Novel insights into mixotrophic cultivation of *nitzschia laevis* for co-production of fucoxanthin and eicosapentaenoic acid. *Bioresource Technol.* 294, 122145. doi: 10.1016/j.biortech.2019.122145
- Lu, X., Sun, H., Zhao, W., Cheng, K.-W., Chen, F., and Liu, B. (2018). A hetero-photoautotrophic two-stage cultivation process for production of fucoxanthin by the marine diatom *nitzschia laevis*. *Mar. Drugs* 16 (7), 219. doi: 10.3390/md16070219
- Mikami, K., and Hosokawa, M. (2013). Biosynthetic pathway and health benefits of fucoxanthin, an algae-specific xanthophyll in brown seaweeds. *Int. J. Mol. Sci.* 14 (7), 13763–13781. doi: 10.3390/ijms140713763
- Peng, J., Yuan, J.-P., Wu, C.-F., and Wang, J.-H. (2011). Fucoxanthin, a marine carotenoid present in brown seaweeds and diatoms: metabolism and bioactivities relevant to human health. *Mar. Drugs* 9 (10), 1806–1828. doi: 10.3390/md9101806
- Perez-Garcia, O., Escalante, F. M. E., de-Bashan, L. E., and Bashan, Y. (2011). Heterotrophic cultures of microalgae: metabolism and potential products. *Water Res.* 45 (1), 11–36. doi: 10.1016/j.watres.2010.08.037
- Sun, H., Li, X., Ren, Y., Zhang, H., Mao, X., Lao, Y., et al. (2020a). Boost carbon availability and value in algal cell for economic deployment of biomass. *Bioresource Technol.* 300, 122640. doi: 10.1016/j.biortech.2019.122640
- and Technology Innovation Commission of Shenzhen (KQTD20180412181334790), and the Shenzhen Science and Technology R & D Fund (20220809171532001).

Conflict of interest

The authors declare that the research was conducted in the absence of any commercial or financial relationships that could be construed as a potential conflict of interest.

Publisher's note

All claims expressed in this article are solely those of the authors and do not necessarily represent those of their affiliated organizations, or those of the publisher, the editors and the reviewers. Any product that may be evaluated in this article, or claim that may be made by its manufacturer, is not guaranteed or endorsed by the publisher.

Sun, H., Ren, Y., Lao, Y., Li, X., and Chen, F. (2020b). A novel fed-batch strategy enhances lipid and astaxanthin productivity without compromising biomass of *chromochloris zofingiensis*. *Bioresource Technol.* 308, 123306. doi: 10.1016/j.biortech.2020.123306

Sun, H., Wu, T., Chen, S. H. Y., Ren, Y., Yang, S., Huang, J., et al. (2021). Powerful tools for productivity improvements in microalgal production. *Renewable Sustain. Energy Rev.* 152, 111609. doi: 10.1016/j.rser.2021.111609

Sun, H., Yang, S., Zhao, W., Kong, Q., Zhu, C., Fu, X., et al. (2022). Fucoxanthin from marine microalgae: a promising bioactive compound for industrial production and food application. *Crit. Rev. Food Sci. Nutr.* 1–17. doi: 10.1080/10408398.2022.2054932

Wang, S., Verma, S. K., Said, I. H., Thomsen, L., Ullrich, M. S., and Kuhnert, N. (2018). Changes in the fucoxanthin production and protein profiles in *cylindrotheca closterium* in response to blue light-emitting diode light. *Microbial Cell Factories* 17, 110. doi: 10.1186/s12934-018-0957-0

Wang, Y., Wang, J., Gu, Z., Yang, S., He, Y., Mou, H., et al. (2023). Altering autotrophic carbon metabolism of *nitzschia closterium* to mixotrophic mode for high-value product improvement. *Bioresource Technol.* 371, 128596–128596. doi: 10.1016/j.biortech.2023.128596

Wang, W., Yu, L.-J., Xu, C., Tomizaki, T., Zhao, S., Umena, Y., et al. (2019). Structural basis for blue-green light harvesting and energy dissipation in diatoms. *Science* 363 (6427), 598–599. doi: 10.1126/science.aav0365

Wang, W., Zhao, S., Pi, X., Kuang, T., Sui, S.-F., and Shen, J.-R. (2020). Structural features of the diatom photosystem II-light-harvesting antenna complex. *FEBS J.* 287 (11), 2191–2200. doi: 10.1111/febs.15183

Wen, Z. Y., and Chen, F. (2000). Production potential of eicosapentaenoic acid by the diatom *nitzschia laevis*. *Biotechnol. Lett.* 22 (9), 727–733. doi: 10.1023/a:1005666219163

Xue, J., Balamurugan, S., Li, D.-W., Liu, Y.-H., Zeng, H., Wang, L., et al. (2017). Glucose-6-phosphate dehydrogenase as a target for highly efficient fatty acid biosynthesis in microalgae by enhancing NADPH supply. *Metab. Eng.* 41, 212–221. doi: 10.1016/j.ymben.2017.04.008

Yi, Z., Su, Y., Cherek, P., Nelson, D. R., Lin, J., Rolfsson, O., et al. (2019). Combined artificial high-silicate medium and LED illumination promote carotenoid accumulation in the marine diatom *phaeodactylum tricornutum*. *Microbial Cell Factories* 18 (1). doi: 10.1186/s12934-019-1263-1

Yoo, K., Antoniewicz, M. R., Stephanopoulos, G., and Kelleher, J. K. (2008). Quantifying reductive carboxylation flux of glutamine to lipid in a brown adipocyte cell line. *J. Biol. Chem.* 283 (30), 20621–20627. doi: 10.1074/jbc.M706494200

Zarekarizi, A., Hoffmann, L., and Burritt, D. (2019). Approaches for the sustainable production of fucoxanthin, a xanthophyll with potential health benefits. *J. Appl. Phycology* 31 (1), 281–299. doi: 10.1007/s10811-018-1558-3

Zhang, R., Kong, Z., Chen, S., Ran, Z., Ye, M., Xu, J., et al. (2017). The comparative study for physiological and biochemical mechanisms of *thalassiosira pseudonana* and *chaetoceros calcitrans* in response to different light intensities. *Algal Research-Biomass Biofuels Bioproducts* 27, 89–98. doi: 10.1016/j.algal.2017.08.026

Zhang, Z., Sun, D., Cheng, K.-W., and Chen, F. (2021). Investigation of carbon and energy metabolic mechanism of mixotrophy in *chromochloris zofingiensis*. *Biotechnol. Biofuels* 14 (1), 36. doi: 10.1186/s13068-021-01890-5

Zhao, L., Zhang, H., Wang, L., Chen, H., Chen, Y. Q., Chen, W., et al. (2015). ¹³C-metabolic flux analysis of lipid accumulation in the oleaginous fungus *mucor circinelloides*. *Bioresour. Technol.* 197, 23–29. doi: 10.1016/j.biortech.2015.08.035